Influence of Instrumented Mouthguard Pre-trigger Time and Post-Trigger Time in Evaluating Brain Strain and Strain Rate in American Football Head Impacts

Nicholas J. Cecchi, Yuzhe Liu, August G. Domel, Michael Zeineh, Gerald Grant, David B. Camarillo

I. INTRODUCTION

In American football, head impacts have the potential to cause mild traumatic brain injury (mTBI), which induces brain deficits and neurological changes. The rapid rotation of the skull during head impact can cause large brain strain and strain rate, which are associated with brain tissue pathology [1]. Therefore, the relationship between head kinematics and brain deformation has been investigated to understand the biomechanics of mTBI. To measure head kinematics in on-field game play, several instrumented mouthguards, containing accelerometers and gyroscopes, have been developed and used to collect head impact data [2-5]. During a head impact, the sensor is typically triggered when the absolute value of linear acceleration at the accelerometer exceeds a threshold value. The 6-DoF kinematics within the sensor's time window (between the pre-trigger time and post-trigger time) will subsequently be recorded. To relate head kinematics to the risk of brain injury, brain strain and strain rate can be calculated by finite element (FE) head model, and the propagation of error in mouthguard measurements to FE simulation has been investigated. Despite the inaccuracy of the sensor measurement, the time window of measurements will influence the FE simulation results because the brain deformation depends on history and the devices are triggered by linear acceleration while the brain strain and strain rate are caused by head rotation [6]. For currently available wearable devices that detect head impacts, pre-trigger and post-trigger times vary widely. Therefore, we aim to identify a minimum time window for American football head impact measurement. In this study, we analyzed head kinematics in on-field head impacts with FE head models and investigated the minimum time window needed for accurate brain strain calculation with intentionally truncated data.

Stanford Instrumented Mouthguard

The head impact data used in this study were collected by MiG2.0 devices (Fig. 1(A)) from the Stanford University football team's training and games [7,8]. All impacts were confirmed by both video analysis and the MiG2.0 neural network classifier [9]. This yielded a total of 118 head impacts. All impacts were subconcussive (i.e. no concussion was reported or diagnosed after any of the impacts). In these data, t=0 ms is the MiG2.0 triggering, and t<0 and t>0 indicate the pre-trigger time and the post-trigger time, respectively.

KTH Finite Element Head model

The KTH FE head model was developed by Royal Institute of Technology in Stockholm, Sweden (Fig. 1(B)) [10]. This model was previously validated by cadaver head impact experiments [10]. The skull was assumed to be rigid, since stress waves will not pass through it, and moved according to the measured on-field head kinematics. As a result, the brain would be deformed by its own inertia. Based on the simulation results, we first calculated the 95th percentile maximal principal strain (95% MPS) and 95% maximal principal strain rate (95% MPSR) at each time frame, and then found the peak values over time. The double precision solver was used.

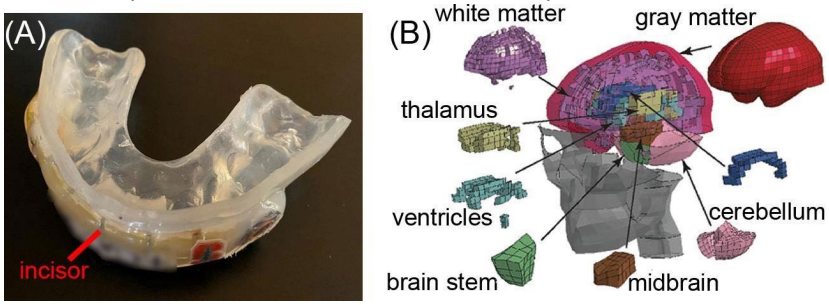

Fig. 1. (A) Stanford Instrumented Mouthguard (MiG2.0). The location of the accelerometer at the incisor is shown. (B) KTH finite element head model.

N. J. Cecchi is a Ph.D. student in Bioengineering, Y. Liu (e-mail: yuzheliu@stanford.edu; tel: +1 612-481-8096) and A. G. Domel are postdoctoral scholars, M. Zeineh is a Professor of Radiology, G. Grant is a Professor of Neurosurgery and D. B. Camarillo is a Professor of Bioengineering, all at Stanford University, California, USA.

Individual Head Difference

To generalize these results across a wide range of athletes, six representative brains in the WU-Minn Human Connectome Project (WUM HCP) [11] were used to study the effect of brain geometry. Since brain strain has been shown to be caused by rotation instead of translation [6] and the momentum of inertia is more influential than mass [12], we scaled the node coordinates of the original KTH model according to the moment of inertia, instead of the brain's mass. For each representative brain, the original KTH model was scaled to have the same moment of inertia about the X axis (posterior to anterior), Y axis (left to right) and Z axis (superior to inferior), with the origin at the brain's center of gravity (CoG).

Pre-Trigger and Post-Trigger Time

To investigate how different pre-trigger and post-trigger times influence brain strain analyses, we performed simulations with intentionally truncated time windows of head kinematics and compared the results with the original brain strain (calculated by the original 200 ms time window of head kinematics). For the pre-trigger time, we started the simulation at -30 ms, -20 ms, -10 ms and 0 ms (triggering) and compared results with the original head kinematics (-50 ms). For the post-trigger time, we calculated the peaks of 95% MPS and 95% MPSR before 30 ms, 40 ms, 50 ms, 60 ms and 70 ms and compared results with the original head kinematics (150 ms). Each group of 95% MPS peaks and 95% MPSR peaks with the same pre-trigger or post-trigger time was tested by Anderson-Darling test for the normality, and then compared with original brain strain by pairwise t-test.

II. INITIAL FINDINGS

Linear Acceleration, Angular Acceleration, Angular Velocity, 95% MPS and 95% MPSR

The peak values of angular acceleration (Fig. 2(A)), angular velocity (Fig. 2(B**)**) and linear acceleration at CoG (Fig. 2(C)) are plotted against their corresponding peak times. Kernel density estimations are plotted at the right and top, respectively. The 95th percentile of peak values (95% peak), the 5th and 95th percentile of peak time (5% and 95% peak time, respectively) are also plotted. In Fig. 2(A) and (B), the peak time for angular acceleration and for linear acceleration at CoG are similar and close to the triggering, while that of the angular velocity is more dispersive, between t=0 ms and t=50 ms. It should also be noted that the kinematics of a few cases reached peaks long before or long after the triggering.

To calculate the 95% MPS and 95% MPSR, the kinematics of the 118 head impacts were input to the seven head models. It was found that 95% MPS and 95% MPSR varied considerably. The peak values and the peak times for the original KTH FE head model are plotted in Fig. 3. Both the 5th and the 95th percentile peak time of 95% MPS are earlier than that of 95% MPSR, and there are small changes in the distribution of the peak time among heads. Similar to the kinematics, the 95% MPS and 95% MPSR peaks long before or long after the triggering in a few cases.

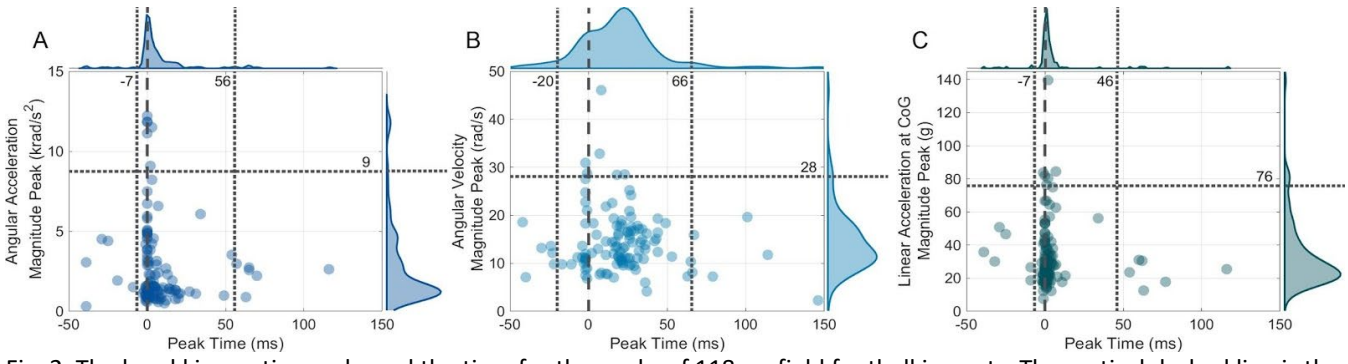

Fig. 2. The head kinematics peaks and the time for the peaks of 118 on-field football impacts. The vertical dashed line is the trigger time (t=0 ms). The left and right vertical dotted lines are the 5th percentile and the 95th percentile of the time for the peaks, respectively, and the horizontal dotted line is the 95th percentile of the head kinematics peaks.

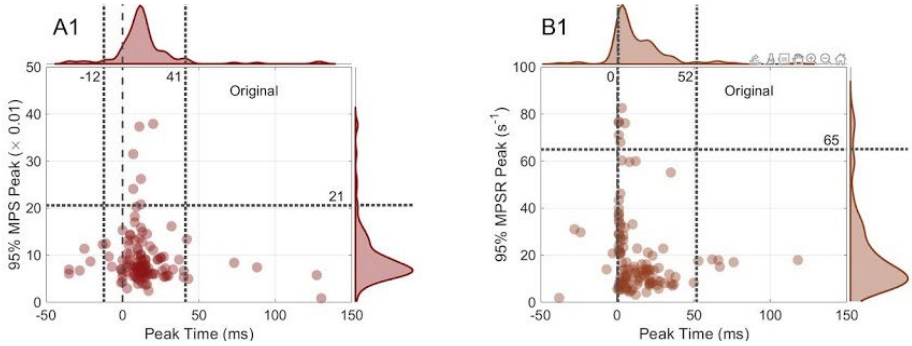

Fig. 3. The 95% MPS and 95% MPSR peaks and the time for the peaks of 118 on-field football impacts. The vertical dashed line is the trigger time (t=0 ms). The left and right vertical dotted lines are the 5th percentile and the 95th percentile of the time for the peaks, respectively, and the horizontal dotted line is the 95th percentile of the head kinematics peaks. The kernel densities of data are plotted at the top and the right of each figure.

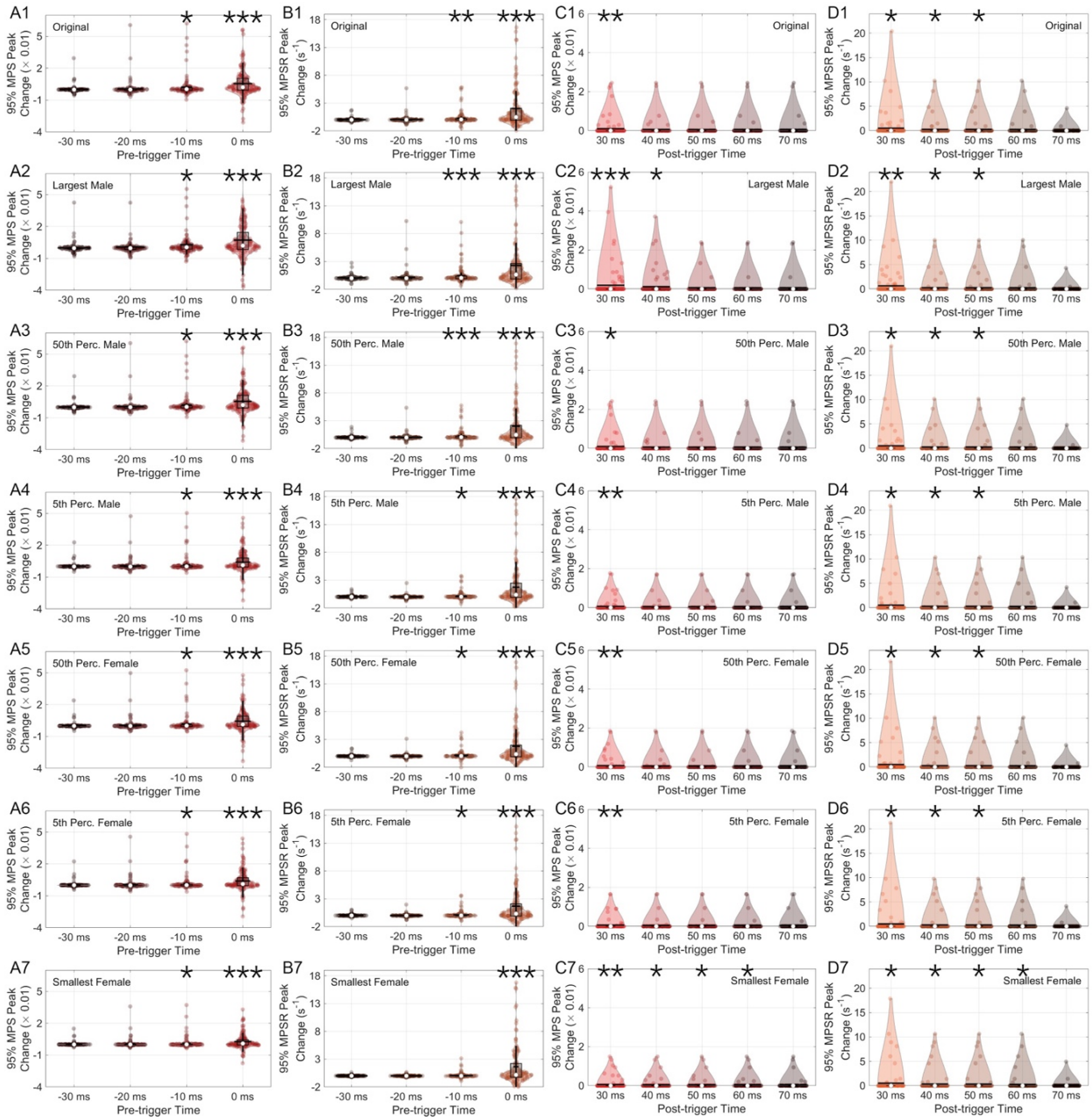

Fig. 4. Violin plots of the changes of 95% MPS and 95% MPSR peaks caused by the pre-trigger and post-trigger time (the results by original data minus the results by new data with different time windows). (A) 95% MPS peak and (B) 95% MPSR peak calculated by different pre-trigger times; (C) 95% MPS peak and (D) 95% MPSR peak calculated by different post-trigger times. (1-7) KTH original and six representative brains. Each group (violin) is compared with the original data (A, B: original pre-trigger time: -50 ms; C, D: original post-trigger time: 150 ms) by pairwise t-test (*:p<0.05, **:p<0.01,

***:p<0.005). In each plot, the shape of violin is the kernel density of the data. (In (C, D), the shape of violin is close to a triangle because the data is always positive). The box plot of each group is shown at the center of each violin.

Difference Caused by Pre-Trigger and Post-Trigger Times

Pre-trigger times were truncated to -30 ms, -20 ms, -10 ms and 0 ms and post-trigger times were truncated to 30 ms, 40 ms, 50 ms, 60 ms and 70 ms. The changes are shown as violin plots (Fig. 4), in which a violin indicates a group of simulation results (118 head impacts) given by the new time window. Each group was confirmed to follow a normal distribution by the Anderson-Darling test and was then compared by pairwise t-test with the simulation results by the original time window of head kinematics. The comparison showed that the pre-trigger time of -20 ms and the post-trigger time of 70 ms are able to give non-significantly different 95% MPS peaks (Fig. 4(A) for pre-trigger, Fig. 4(C) for post-trigger) and 95% MPSR peaks (Fig. 4(B) for pre-trigger, Fig. 4(D) for post-trigger) for all head models.

III. DISCUSSION

In Fig. 2 and Fig. 3, most peaks of the on-field impact kinematics and brain strain occurred soon after the device triggering, and few impacts had peaks much earlier or much later than the triggering. It was also found that peak times for 95% MPS and 95% MPSR are influenced by brain geometry (Fig. 4). To address this, the original KTH head model and six representative head models were used in simulations to observe the effect of brain size on the kinematics. When considering all head models, a time window of [-20 ms, 70 ms] was found to give 95% MPS and 95% MPSR peaks that were non-significantly different from the original data (Fig. 4). Therefore, [-20 ms, 70 ms] is suggested as the minimum time window for recording head kinematic data via instrumented mouthguards.

IV. REFERENCES

[1] O'Keeffe, E., Kelly, E., et al. Dynamic Blood–Brain Barrier Regulation in Mild Traumatic Brain Injury. *Journal of neurotrauma*, 2020. 37(2): p. 347-356

[2] Rowson, S., Beckwith, J.G., et al. A six degree of freedom head acceleration measurement device for use in football. *Journal of applied biomechanics*, 2011. 27(1): p. 8-14

[3] Liu, Y., Domel, A.G., et al. Validation and comparison of instrumented mouthguards for measuring head kinematics and assessing brain deformation in football impacts. *Annals of Biomedical Engineering*, 2020. 48(11): p. 2580-2598

[4] Gabler, L.F., Huddleston, S.H., et al. On-Field Performance of an Instrumented Mouthguard for Detecting Head Impacts in American Football. *Annals of Biomedical Engineering*, 2020: p. 1-14

[5] Bartsch, A., Samorezov, S., Benzel, E., Miele, V., and Brett, D. Validation of an "intelligent mouthguard" single event head impact dosimeter. 2014, SAE Technical Paper.

[6] Ji, S., Zhao, W., Li, Z., and McAllister, T.W. Head impact accelerations for brain strain-related responses in contact sports: a model-based investigation. *Biomechanics and modeling in mechanobiology*, 2014. 13(5): p. 1121-1136

[7] Hernandez, F., Wu, L.C., et al. Six degree-of-freedom measurements of human mild traumatic brain injury. *Annals of biomedical engineering*, 2015. 43(8): p. 1918-1934

[8] Tiernan, S., Meagher, A., et al. Concussion and the severity of head impacts in mixed martial arts. *Proceedings of the Institution of Mechanical Engineers, Part H: Journal of Engineering in Medicine*, 2020: p. 0954411920947850

[9] Domel, A.G., Raymond, S.J., et al. A New Open-Access Platform for Measuring and Sharing mTBI Data. *arXiv preprint arXiv:2010.08485*, 2020

[10] Kleiven, S. Predictors for traumatic brain injuries evaluated through accident reconstructions. 2007, SAE Technical Paper.

[11] Van Essen, D.C., Smith, S.M., et al. The WU-Minn human connectome project: an overview. *Neuroimage*, 2013. 80: p. 62-79

[12] Zou, H., Kleiven, S., and Schmiedeler, J.P. The effect of brain mass and moment of inertia on relative brain–skull displacement during low-severity impacts. *International journal of crashworthiness*, 2007. 12(4): p. 341-353